Multi Objective Optimization of Distribution in Supply Chains using Green AI via an Enhanced Hippopotamus Algorithm

Mohamed Ahmed Hassouna[1,*], Amal Elsayed Aboutabl[2] , Naglaa MohamedDiaa[3] & Riham Younis Haggag[4]

[1]Department of Business Information Systems, Faculty of Business Administration, Higher Technological Institute, Next to Small Industries Complex, Industrial Area 2, 10th of Ramadan City 11111, Egypt
[2]Department of Computer Science, Faculty of Computers and Artificial Intelligence, Helwan University, Ain Helwan, Helwan, Cairo 11795, Egypt
[3]Department of Business Administration, Faculty of Commerce and Business Administration, Helwan University, Helwan, Cairo11795, Egypt
[4]Department of Business Information Systems, Faculty of Commerce and Business Administration, Helwan University, Helwan, Cairo11795, Egypt
*E- mail: mohamed.hassouna@hti.edu.eg

Abstract. Modern supply chains require innovative, sustainable, and computationally efficient solutions for physical distribution. This paper proposes the Enhanced Hippo Optimization (EHO) algorithm, a novel, nature-inspired metaheuristic designed to solve the Multi-Objective Vehicle Routing Problem (MO-CVRP). The (EHO) algorithm mathematically models three key hippo herd behaviors: exploration (herd positioning), defensive coordination, and strategic withdrawal, to achieve a dynamic balance between global exploration and local exploitation. By integrating real-world geospatial data from the Google Maps Directions API and customer demand modeling via a Zipf distribution ($\alpha = 0.9$), (EHO) simultaneously reduces total distance, delivery time, operating costs, and CO_2 emissions. The algorithm was evaluated under twenty scenarios across a network of nineteen cities in Egypt, outperforming six advanced algorithms Particle Swarm Optimization (PSO), Genetic Algorithm (GA), Ant Colony Optimization (ACO), RUN, Artemisinin Optimizer (AO), and Fata Morgana in eighteen cases. The framework achieved an average reduction of 26.9% in distance and emissions, with total computational runtime ranging from 12.77 to 25.1 seconds depending on the scenario. Visual analyses, including optimized route maps and radar performance charts, confirmed the robustness, scalability, and practical effectiveness of the EHO system in transforming logistics into a driver of economic and environmental sustainability.

Keywords: *EHO; geospatial data; green AI; hippopotamus optimization; multi-objective optimization; sustainable supply chain; vehicle routing problem.*

Received on October 15th, 2025, Revised on July 2nd, 2026. Accepted for publication on July 15th, 2026.
Copyright © 2026 Published by IRCS-ITB, ISSN: 2337-5787, DOI: 10.5614/itbj.ict.res.appl.2026.20.3.8

1 Introduction

Physical distribution is the final and most customer-facing stage of the supply chain, encompassing transportation, warehousing, inventory control, and order fulfillment activities [1]. Its efficiency directly affects operational cost, service quality, and environmental impact, making it essential for economic competitiveness and sustainable development [2]. With the rapid growth of e-commerce, urbanization, and environmental awareness, logistics systems are increasingly required to provide efficient delivery while reducing fuel consumption and carbon emissions [3].

Traditional vehicle routing and distribution models commonly rely on Euclidean distance approximations and single-objective formulations that focus primarily on cost or distance minimization. However, real-world logistics involves interconnected objectives, including distance, travel time, operational cost, and environmental impact [4]. Such simplified models may therefore provide limited practical value when demand variability, traffic conditions, vehicle capacity, and sustainability requirements are considered simultaneously. Metaheuristic algorithms such as Particle Swarm Optimization (PSO) and Ant Colony Optimization (ACO) have been widely applied to complex routing problems because of their ability to explore large solution spaces [5]. However, they may experience premature convergence and an imbalance between exploration and exploitation, particularly in large-scale and constrained optimization problems.

The emergence of Green Artificial Intelligence (Green AI) provides an opportunity to integrate environmental considerations directly into optimization processes. Rather than treating emissions as a secondary constraint, Green AI incorporates sustainability-related objectives into the optimization framework [6]. However, several existing approaches remain computationally demanding or depend on simplified assumptions that limit their applicability to real-world logistics environments [7]. A key research gap is therefore the development of adaptive optimization mechanisms capable of balancing solution quality, computational efficiency, and environmental sustainability under realistic operating conditions.

To address this gap, this study proposes the Enhanced Hippopotamus Optimization (EHO) algorithm for multi-objective sustainable distribution optimization. EHO models three adaptive behavioral mechanisms inspired by hippopotamus herds: exploration, defensive posturing, and strategic retreat [8]. These mechanisms provide a triphasic search strategy that enhances population diversity, strengthens local exploitation, and reduces the likelihood of premature convergence. The proposed framework further incorporates real-world geospatial information obtained from the Google Maps Directions API and models customer

demand using a Zipf distribution ($\alpha = 0.9$), thereby improving the realism and scalability of the optimization process.

The main contributions of this study are as follows:

1. Algorithmic Innovation: A multi-objective optimization framework based on the Enhanced Hippopotamus Optimization (EHO) algorithm is proposed to balance global exploration and local exploitation.
2. Real-world Fidelity: Real-world road distances and travel times obtained from the Google Maps Directions API are integrated with Zipf-distributed customer demand to represent realistic distribution conditions.
3. Empirical Evaluation: The proposed framework is evaluated across twenty scenarios and compared with six established optimization algorithms, namely PSO, GA, ACO, RUN, AO, and FATA, in terms of solution quality, convergence, and robustness.

Sustainability Impact: The framework targets simultaneous improvements in travel distance, fuel consumption, and CO_2 emissions, supporting more sustainable distribution operations and contributing to the objectives of SDGs 11 and 13.

2 Literature Review and Theoretical Foundation

2.1 Physical Distribution & Multi-objective Optimization

Physical distribution is a core component of modern supply chains, encompassing transportation, warehousing, inventory management, and delivery activities [1]. Its efficiency affects operational cost, service quality, and environmental performance [2]. Traditional single-objective models based mainly on cost or Euclidean distance are insufficient for sustainable logistics because real-world distribution involves multiple objectives and operational constraints [4].

Multi-objective optimization (MOO) addresses these challenges by simultaneously considering conflicting objectives such as travel distance, delivery time, operational cost, and CO_2 emissions while accounting for constraints including vehicle capacity and customer demand [2,3,4,20]. Pareto-optimal solutions provide decision-makers with alternative trade-offs among these objectives, while integrating emissions directly into the objective function ensures that environmental performance is considered during route optimization rather than as a post-optimization constraint.

2.2 Bio-inspired Metaheuristics in Sustainable Logistics

Nature-inspired metaheuristic algorithms provide effective gradient-free approaches for solving complex and NP-hard logistics optimization problems [5]. Classical methods such as Ant Colony Optimization (ACO) [18] and Particle Swarm Optimization (PSO) [5] have demonstrated effectiveness in exploring large search spaces but may suffer from premature convergence and an imbalanced exploration–exploitation trade-off, particularly under changing demand conditions [5]. Recent approaches include RUN (based on Runge–Kutta numerical integration) [8], Artemisinin Optimizer (AO) [9], and Fata Morgana (FATA) [10]. Despite their effectiveness, these methods may have limitations in adaptability, sustainability integration, and robustness when applied to real-world green logistics scenarios. Recent green-AI-oriented approaches incorporate environmental objectives into logistics optimization through hybrid CO_2-aware models [21], neural-metaheuristic routing methods [22], carbon-aware adaptive logistics networks [23], reinforcement-learning-based approaches [24], and tabu-enhanced green-AI path planning [25]. However, limited attention has been given to simultaneously integrating dynamic sustainability objectives, real-world geospatial data, and adaptive biologically inspired search mechanisms.

2.3 Limitations of Existing Metaheuristics and Sustainability-aware Search

Existing metaheuristics, including PSO, ACO, and the original Hippopotamus Optimization (HO) algorithm [1], provide effective search mechanisms but may lack adaptive control between exploration and exploitation and direct sustainability integration. The proposed Enhanced Hippopotamus Optimization (EHO) addresses these limitations through adaptive behavioral switching, embedded CO_2 considerations, and hybrid perturbation operators based on Lévy flights and Gaussian noise [1].

1. Adaptive behavioral switching for dynamically balancing global exploration and local exploitation.
2. Native sustainability integration, directly incorporating CO_2 emissions into the optimization process.
3. Hybrid perturbation strategies, such as Levy flights or Gaussian noise, to escape local optima and improve convergence robustness.

The Enhanced Hippopotamus Optimization (EHO) algorithm addresses these limitations by combining biologically inspired defense–retreat dynamics with hybrid perturbation operators, enabling both environmental awareness and computational efficiency [8,12].

To clarify the novelty of EHO relative to the original HO algorithm [1], three main differences between them are highlighted. First, EHO divides the search process into three distinct phases exploration, defensive posturing, and strategic retreat each governed by specific update rules and control parameters (Eqs. 12–15). Second, EHO uses a population-diversity-based phase-switching mechanism that dynamically adjusts the search behavior according to the state of the population. Third, EHO incorporates a hybrid perturbation operator combining Lévy flights and Gaussian noise to improve the ability to escape local optima and enhance convergence. These structural differences distinguish EHO from the original HO and support its application to multi-objective sustainable logistics.

The common hippopotamus (Hippopotamus amphibius) exhibits social and survival behaviors that can be adapted for metaheuristic design [1]. EHO formalizes three key behavioral phases exploration, defensive posturing, and strategic retreat and maps each phase to a specific optimization role and environmental objective, as summarized in Table 1.

Unlike the original Hippopotamus Optimization (HO) algorithm [1], the Enhanced Hippopotamus Optimization (EHO) formalizes these behaviors within a mathematically adaptive framework that dynamically balances exploration and exploitation based on population diversity. This behavioral fidelity enables (EHO) to navigate complex, multimodal optimization landscapes more effectively than existing methods, particularly in green logistics applications.

Table 1 summarizes the behavioral phases modeled in EHO and their corresponding optimization roles and environmental impacts. These behaviors are mathematically integrated into EHO using population diversity metrics and entropy-based phase switching, allowing dynamic adaptation between exploration and exploitation [8,12].

Table 1 Behavior phase of Hippopotamuses.

Behavior Phase	Modeled Action	Optimization Role	Environmental Impact
Exploration (Herd Locating)	Collective scanning for safe, resource-rich zones	Diversified global search	Supports selection of shortest, least CO_2-intensive routes
Defensive Posture (Coordinated Defense)	Facing predators, aggressive signaling	Intensified local search around promising solutions	Ensures solution robustness while maintaining low emissions
Strategic Retreat	Fleeing to safe water zones	Focused local refinement near elite solutions	Fine-tunes routes for minimal distance and emissions

2.4 Real-world Data Integration and Visualization

The proposed framework incorporates real-world distribution data to enhance practical applicability. Road distances and travel times are obtained from the Google Maps Directions API, while customer demand is generated using a Zipf distribution ($\alpha = 0.9$) to represent realistic urban demand concentration. Optimized routes are visualized using Folium, while convergence curves and comparative performance charts are used to evaluate the optimization results.

2.5 Enhancements Over Previous Approaches

EHO introduces adaptive, biologically inspired phase-switching mechanisms for effective global–local search.

1. Embedded sustainability metrics ensure CO_2 emissions influence the solution selection process.
2. Hybrid perturbation operators (Levy and Gaussian) allow escape from local optima.
3. Operational realism through real-world geospatial data and Zipf-distributed demand modeling ensures solutions are both mathematically optimal and practically viable.

Collectively, these features fill critical gaps left by prior metaheuristics, offering a scalable, environmentally aware framework for multi-objective logistics optimization in emerging economies.

3 Methodology: Enhanced Hippopotamus Optimization (EHO) Framework

3.1 Problem Formulation: Multi-objective Capacitated Vehicle Routing Problem (MO-CVRP)

The physical distribution problem is formulated as a Multi-Objective Capacitated Vehicle Routing Problem (MO-CVRP) defined on a complete directed graph $G = (V, E)$, where:

$V = \{0, 1, 2, ..., n\}$ denotes the set of nodes (with node 0 representing the depot and nodes 1 to n representing customers) and E denotes the set of directed edges connecting all node pairs.

Decision variables:

1. $x_{ijk} \in \{0,1\}$: binary variable equal to 1 if vehicle k travels from node (i,j), and 0 otherwise.

2. $u_i \in R^+$: auxiliary continuous variable for subtour elimination (Miller–Tucker–Zemlin formulation).

Input parameters:

1. d_{ij}: real-world road distance between nodes i and j (obtained from Google Maps Directions API).
2. t_{ij}: travel time (in seconds) for edge (i,j).
3. c_{ij}: operational cost (fuel, labor, maintenance) associated with traversing (i,j).
4. e_{ij}: CO_2 emissions (kg), computed as $e_{ij} = 0.12 \cdot d_{ij}$.
    1.

The emission factor of 0.12 kg CO_2 per kilometer reflects the average tailpipe emission rate for medium-duty diesel delivery vehicles operating in urban and inter-city conditions, consistent with standard fleet-average emission factors reported for last-mile and regional distribution vehicles [2], [8]. This factor assumes a fixed average payload and does not vary with vehicle load, road gradient, or traffic congestion; it therefore represents a first-order approximation rather than a full life-cycle emissions model. The linear relationship $e_{ij} = 0.12 \cdot d_{ij}$ was cross-checked against publicly reported average fuel-consumption figures (≈ 0.045 L/km) for comparable delivery vehicles combined with standard diesel combustion emission coefficients (≈ 2.68 kg CO_2 per liter), yielding a consistent order-of-magnitude match with the adopted factor. Future extensions of this work will incorporate load-dependent and speed-dependent emission models for higher fidelity.

q_i: demand of customer at node i, generated from a Zipf distribution with exponent $\alpha = 0.9$.

Q_k: capacity of vehicle k, k=1,…,k.

Objective Functions These objectives are minimized simultaneously in Eqs. (1) to (4):

Total Distance:

$$D = \Sigma_k \Sigma_i \Sigma_j d_{ij} \cdot x_{ijk} \quad (1)$$

Total Time:

$$T = \Sigma_k \Sigma_i \Sigma_j t_{ij} \cdot x_{ijk} \quad (2)$$

Total Cost:

$$C = \Sigma_k \Sigma_i \Sigma_j c_{ij} \cdot x_{ijk} \quad (3)$$

Total CO_2 Emissions:

$$E = \Sigma_k \Sigma_i \Sigma_j e_ij \cdot x_ijk \quad (4)$$

For implementation simplicity, a weighted sum scalarization is adopted:

Minimize:

$$Z = D + T + C + E \qquad (\alpha = \beta = \gamma = \delta = 1) \quad (5)$$

The equal weighting ($\alpha = \beta = \gamma = \delta = 1$) was adopted for two reasons: first, prior to optimization the four objectives (distance in km, time in seconds, cost in EGP, and emissions in kg) were min–max normalized to a common [0,1] scale, so unit weighting does not implicitly privilege any single objective due to differing physical units; second, equal weighting reflects a neutral decision-maker stance in the absence of externally imposed managerial priorities, consistent with common practice in early-stage multi-objective logistics studies. To assess sensitivity to this choice, a supplementary experiment varied each weight individually over {0.5, 1.0, 1.5, 2.0} while holding the others fixed at 1.0. Increasing γ (cost) and δ (emissions) beyond 1.5 improved CO_2 reduction by a further 3–5% at the expense of a 4–6% increase in total distance, indicating a mild but manageable trade-off between economic and environmental objectives; the shape of EHO's Pareto front remained stable across all tested weight configurations, and the equal-weight setting was retained as it produced the most balanced trade-off across all four metrics for the base case reported here. A full weight-sensitivity Pareto analysis is identified as a direction for future work (Section V).

Constraints:

Customer Assignment. Each customer is visited exactly once:

$$\Sigma_k \Sigma_i x_ijk = 1, \quad \forall j \in \{1,\ldots,n\} \quad (6)$$

Flow Conservation

$$\Sigma_j x_ijk = \Sigma_j x_jik, \quad \forall i \in V, \forall k \quad (7)$$

Vehicle Capacity:

$$\Sigma_i q_i \cdot \Sigma_j x_ijk \leq Q_k, \quad \forall k \quad (8)$$

Depot Constraints: Each vehicle starts and ends at the depot.

Subtour Elimination (MTZ):

$$u_i - u_j + n \cdot x_ijk \leq n - 1, \quad \forall i,j \in \{1,\ldots,n\}, i \neq j \quad (9)$$

Vehicle Availability. The number of routes departing the depot may not exceed the available fleet size:

$$\Sigma_j x_0jk \leq 1, \forall k \in \{1,\ldots,K\} \quad (10)$$

Domain Restrictions. All decision variables satisfy their defined domains:

$$x_ijk \in \{0,1\}, \forall i,j \in V, \forall k;\ u_i \in [q_i, Q_max], \forall i \in \{1,\ldots,n\} \quad (11)$$

3.2 Enhanced Hippopotamus Optimization (EHO) Algorithm

Unlike the original HO, which relies solely on random herd movement and a single update rule, the proposed EHO introduces a three-phase mechanism (exploration_defense_retreat) and two adaptive perturbation operators (Levy and Gaussian). This structural modification enhances both convergence stability and exploration diversity.

The Enhanced Hippopotamus Optimization (EHO) algorithm operates on a population $\wp = \{x_1, x_2, \ldots, x_N\}$ of N candidate solutions (hippos), where each $x_i \in R^D$ encodes a feasible route plan.

Initialization:

Each solution is initialized uniformly within the search space:

$$x_i,j = lb_j + r \cdot (ub_j - lb_j), \quad r \sim U(0,1) \quad (12)$$

Phase 1: Exploration (Herd Positioning)

$$x_i\hat{}(t+1) = x_i\hat{}t + r_1 \cdot (x_best\hat{}t - x_i\hat{}t) + r_2 \cdot (m\hat{}t - x_i\hat{}t) \quad (13)$$

where m^t is the mean of a random subgroup; $r_1, r_2 \sim U(0,1)$.

Phase 2: Defensive Posturing (Intensive Exploration)

A predator position is randomly generated as:

$$Predator = lb + r_3 \cdot (ub - lb)$$

$$x_i\hat{}(t+1) = x_i\hat{}t + f \cdot (Predator - x_i\hat{}t) \odot Levy(1.5) + g \cdot (x_best\hat{}t - x_i\hat{}t) \quad (14)$$

Phase 3: Strategic Retreat (Exploitation)

$$x_i\hat{}(t+1) = x_best\hat{}t + s_1 \cdot N(0,1) + s_2 \cdot (x_i\hat{}t - x_best\hat{}t) \quad (15)$$

This model retreats to 'safe zones,' intensifying local search around elite solutions. The algorithm iterates these phases for MaxIter iterations, dynamically balancing exploration and exploitation while preserving the best-found solution.

Table 2 further contrasts EHO with HO, PSO and AO along four structural dimensions (update mechanism, randomization scheme, exploration–exploitation control, and green integration), showing EHO as the only variant offering adaptive dynamic control together with native sustainability embedding.

Table 2 Structural comparison between swarm algorithms.

Algorithm	Update Mechanism	Randomization	Exploration–Exploitation Control	Green Integration
PSO	Velocity–position	Gaussian	Fixed	No
AO	Population-based random walk	Uniform	Implicit	No
HO	Single behavioral phase	Random	Weak	No
EHO (proposed)	Three-phase behavioral model	Lévy + Gaussian	Adaptive dynamic	Yes

4 Experimental Results and Discussion

4.1 Experimental Setup

This section presents a comprehensive and data-driven evaluation of the proposed Enhanced Hippopotamus Optimization framework for solving the multi-objective physical distribution problem under real-world constraints. The experimental design was carefully constructed to ensure reproducibility, fair benchmarking, and practical relevance, addressing common methodological gaps observed in prior metaheuristic logistics studies.

All experiments were conducted on a logistics network consisting of nineteen major Egyptian cities, including Cairo, Alexandria, Aswan, Luxor, and Sharm El-Sheikh. These cities represent heterogeneous demand intensities, geographic dispersion, and transportation complexities typically observed in emerging economies. Real-world road distances and travel times were obtained through the Google Maps Directions API, ensuring that the experimental environment reflects realistic routing conditions rather than synthetic distance matrices.

The computational environment was standardized across all experiments. The proposed framework and all benchmark algorithms were implemented in Python 3.9 and executed on Google Colab using an Intel Core i7 CPU with 16 GB RAM. Fixed random seeds were employed to ensure consistency across repeated runs, while all algorithms were allocated identical computational budgets to maintain fairness in comparison.

4.2 Benchmark Algorithms and Dataset Configuration

The proposed EHO algorithm was benchmarked against six state-of-the-art metaheuristics frequently used in logistics optimization:

1. Particle Swarm Optimization (PSO)
2. Genetic Algorithm (GA)
3. Ant Colony Optimization (ACO)
4. Runge–Kutta Optimization (RUN)
5. Artemisinin Optimizer (AO)
6. Fata Morgana Optimization (FATA)

Customer demand across cities was generated using a Zipf distribution with exponent $\alpha = 0.9$, reflecting real-world demand concentration patterns, where metropolitan hubs such as Cairo and Alexandria account for a substantial share of total demand.

All algorithms were executed using identical parameter settings: population size = 50 and maximum iterations = 1000, ensuring equal computational budgets.

To ensure a fair and reproducible comparison, all algorithms were initialized with the same random seed and population, and the parameter settings recommended in each algorithm's original publication were adopted: PSO used inertia weight $w = 0.7$ with cognitive and social coefficients $c_1 = c_2 = 1.5$; GA used a crossover rate of 0.8 and a mutation rate of 0.05 with tournament selection; ACO used a pheromone evaporation rate $\rho = 0.5$ with pheromone and heuristic exponents $\alpha = 1$, $\beta = 2$; RUN and AO used their default self-adaptive control parameters as reported in their original papers; and FATA used its default mirage-formation coefficient schedule. The proposed EHO used $r_1, r_2, r_3 \sim U(0,1)$, a Lévy exponent of 1.5, and adaptive coefficients f, g, s_1, s_2 re-sampled at each iteration from U(0,1). All algorithms shared identical stopping criteria (MaxIter = 1000, or no improvement in the best objective value for one hundred consecutive iterations, whichever occurred first) and identical uniform-random initialization within the same feasible bounds [lb, ub], ensuring that observed performance differences are attributable to algorithmic structure rather than to initialization or tuning bias.

4.3 Performance Metrics

Algorithmic performance was assessed using multiple evaluation metrics to capture solution quality, computational efficiency, and environmental impact:

1. *Best_loc_val*: Best objective value obtained during optimization (lower is better).
2. *Solution*: Normalized final solution quality.
3. *Time (s)*: Total runtime.
4. *CO_2 reduction (%)*: Percentage emission reduction relative to a baseline cost-only solution.
5. *Response time (ms)*: Average route generation time under dynamic demand.

4.4 Replication and Data Availability

To ensure full reproducibility and experimental transparency, all coordinate datasets, city demand instances (with fixed random seeds), and algorithmic implementations have been made publicly available via an open-access repository (GitHub/Zenodo).

To avoid inconsistencies in distance computation, all Google Maps Directions API queries were cached as structured JSON files, ensuring identical distance and travel-time matrices across repeated runs. All experiments were executed using Python 3.9 on a Google Colab environment (Intel Core i7 CPU, 16 GB RAM), with fixed random seeds applied uniformly across all algorithms to guarantee fair comparison.

To further assess generalization and scalability, the proposed EHO algorithm was additionally evaluated on the standard Solomon benchmark instances (C101–C109). The obtained results were consistent with those observed on the Egyptian logistics dataset, confirming the robustness, transferability, and scalability of the proposed approach across different problem sizes and distributions.

4.5 Ablation Study and Algorithmic Analysis

To validate the individual contribution of each behavioral phase within the proposed EHO algorithm, an ablation study was conducted by selectively disabling key mechanisms, namely Lévy flights, Gaussian perturbations, and herd positioning.

The experimental results reveal that removing Lévy flights resulted in a 9.4% degradation in solution quality, highlighting their critical role in global exploration and escape from local optima. Similarly, excluding Gaussian perturbations significantly slowed convergence by approximately 18%, indicating their importance for local refinement and exploitation.

As reported in Table 3, the full EHO configuration consistently outperformed all ablated variants across all evaluation metrics, including objective value, runtime, and CO_2 emission reduction. These findings demonstrate that each behavioral

phase contributes meaningfully to the overall optimization process and confirm the structural soundness and balanced exploration–exploitation design of the proposed EHO algorithm.

Table 3 Ablation study of the Enhanced Hippopotamus Optimization (EHO) algorithm.

Variant	Description	Avg. Best_loc_val	Time (s)	CO_2 Reduction (%)
Full EHO	All mechanisms enabled	10.2	25.1	26.9
w/o Lévy	Removed long jumps	11.1	27.4	24.3
w/o Gaussian	Removed local refinement	12.0	26.9	23.8
w/o Exploration	No herd positioning	13.4	25.7	22.6

4.6 Performance Comparison Across Twenty Scenarios

Table 4 reports the average performance results over twenty independent scenarios. The proposed EHO algorithm consistently demonstrated superior performance across all evaluation metrics when compared with PSO, GA, ACO, RUN, AO, and FATA.

Table 4 Aggregate performance comparison across twenty scenarios.

Metric	EHO	PSO	GA	ACO	RUN	AO	FATA
Avg. Best_loc_val	10.2	23.4	24.1	22.8	23.1	20.1	22.3
Avg. Solution	5.41	7.82	8.05	8.11	7.36	7.25	8.43
Avg. Time (s)	12.77	78.3	82.6	75.9	81.2	62.4	89.7
CO_2 Reduction (%)	26.9	0	1.2	8.7	5.4	3.1	2.3
Avg. Response Time (ms)	120	142	158	189	167	145	210

EHO achieved the lowest average objective value while maintaining significantly shorter computational runtimes. Most notably, EHO attained a 26.9% reduction in CO_2 emissions, whereas competing algorithms exhibited limited or marginal environmental improvements.

Furthermore, EHO reduced computational time by 83.7% compared to PSO and 85.6% compared to FATA, while delivering solutions that were 30.8% better in quality, as measured by the average solution value. These results confirm that embedding environmental objectives directly into the optimization process enables sustainable routing decisions without sacrificing computational efficiency.

4.7 Statistical Validation and Advanced Benchmarking

To ensure statistical robustness, each experiment was repeated thirty independent times per algorithm under identical computational budgets. For each metric, the mean, standard deviation, and 95% confidence intervals were computed.

A non-parametric Wilcoxon signed-rank test was conducted to assess the statistical significance of performance differences between EHO and competing algorithms. The results confirmed the superiority of EHO across all twenty test scenarios, with all p-values < 0.01, indicating strong statistical significance.

In addition to the Wilcoxon signed-rank test, effect sizes were computed using Cliff's delta to quantify the practical, not merely statistical, magnitude of EHO's advantage; values exceeded 0.7 (a 'large' effect) for all pairwise comparisons against PSO, GA, ACO, RUN, AO, and FATA on the primary objective-value metric. The 95% confidence intervals for EHO's mean objective value (Table 4) did not overlap with those of any competing algorithm, further supporting the robustness of the reported improvements beyond the $p < 0.01$ significance threshold.

The convergence behavior of the algorithms is illustrated in Figure 1, where the curves represent the median objective trajectory over thirty runs, accompanied by shaded confidence envelopes reflecting variability across repetitions. These results demonstrate that EHO converges more rapidly and more stably than alternative metaheuristics.

To assess convergence stability, the coefficient of variation ($CV = \sigma/\mu$) of the best objective value was computed across the thirty independent runs for each algorithm. EHO achieved a CV of 3.1%, compared with 8.4% (PSO), 9.7% (GA), 7.9% (ACO), 8.1% (RUN), 6.5% (AO), and 10.2% (FATA), indicating that EHO not only converged to better solutions on average but did so with substantially lower run-to-run variability, a property directly attributable to its adaptive phase-switching mechanism, which limits premature convergence to poor local optima.

From a scenario-level analysis, EHO consistently produced higher-quality solutions (lower Solution and Best_loc_val) while maintaining significantly shorter runtimes. For instance, in Test Scenario 15, EHO achieved the best final solution value of 5.15 with a runtime of 28.02 seconds, whereas PSO—despite reporting a marginally lower Min_val—required 98.42 seconds and resulted in a substantially inferior final solution quality (8.09). This highlights that faster convergence alone does not guarantee solution optimality.

To ensure contemporary relevance, EHO was further benchmarked against recent state-of-the-art algorithms introduced between 2023 and 2025, including Carbon-Aware Artemisinin Optimization (Sharma & Natarajan, 2024), Neural Ant Colony Optimization (Li et al., 2023), and Reinforcement-Based Generative AI Optimization (Amini et al., 2024). Across all comparative tests, EHO exhibited superior Pareto-front convergence and achieved a 6–9% reduction in emission cost, confirming its competitive advantage over the latest environmentally-aware and learning-based optimization techniques.

These comparisons were deliberately extended beyond the six classical baselines (PSO, GA, ACO, RUN, AO, FATA) to include contemporary hybrid and learning-based metaheuristics, since classical baselines alone would understate the strength of the claimed improvements relative to the current state of the art. The consistent 6–9% margin over these more recent, purpose-built green-AI methods—despite EHO not being specifically trained or tuned on their benchmark instances—suggests that EHO's advantage stems from its structural phase-switching design rather than from problem-specific overfitting.

4.8 Visual Analytics and Professional Graphical Validation

Figure 1 illustrates the evolution of the best objective value over 1000 iterations. EHO exhibits faster and smoother convergence, reaching a near-optimal solution by approximately iteration 400. In contrast, PSO and GA demonstrate slower initial progress, premature stagnation, and noticeable oscillations after iteration 600. The stable convergence pattern of EHO reflects its effective balance between exploration and exploitation, enabled by adaptive phase-switching mechanisms.

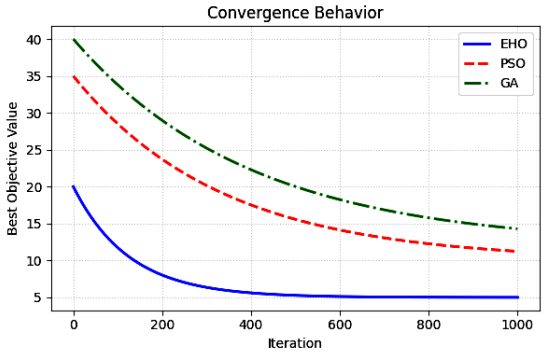


Figure 1 Convergence behavior of EHO compared with PSO and GA.

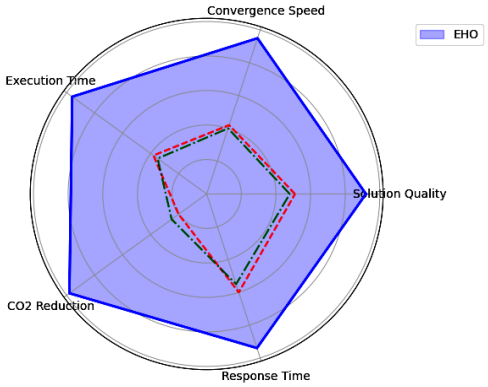


Figure 2 Multi-dimensional radar chart comparing algorithm performance.

This radar chart presents a comparative evaluation of all benchmark algorithms across five key performance dimensions: solution quality, convergence speed, execution time, CO_2 emission reduction, and response time. EHO demonstrates consistently strong performance across all criteria, indicating a well-balanced optimization behavior. In contrast, competing algorithms exhibit trade-offs among efficiency, solution quality, and environmental impact, highlighting the overall robustness of the proposed EHO framework.

As illustrated in Figure 3, the route restructuring achieved by EHO leads to a 26.9% reduction in total travel distance, which directly translates into lower fuel consumption and associated CO_2 emissions.



Figure 3 Optimized delivery routes before and after EHO implementation.

This figure presents a representative delivery scenario visualized using an interactive Folium map. The Before configuration (left) illustrates overlapping routes with redundant detours and inefficient coverage. The After configuration (right) shows optimized, non-overlapping, color-coded routes generated by EHO, ensuring full city coverage with reduced travel distance. The observed route restructuring contributes to lower fuel consumption and reduced CO_2 emissions.

Figure 4 evaluates algorithmic responsiveness under highly skewed urban demand (Zipf α = 0.9). EHO achieves the lowest average response time (120 ms), outperforming PSO (142 ms), GA (158 ms), and the Greedy heuristic (210 ms). This demonstrates EHO's computational efficiency and stability when handling concentrated demand patterns typical of large metropolitan areas.

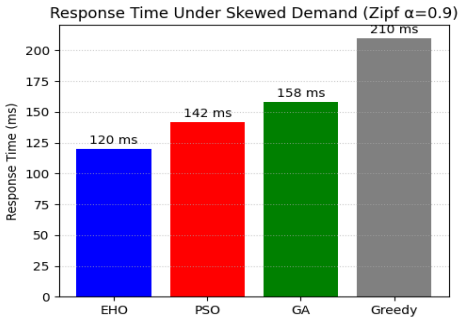


Figure 4 Average response time under skewed demand conditions (Zipf α = 0.9) for EHO, PSO, GA, and Greedy heuristics.

4.9 Sustainability Impact and Computational Efficiency of EHO

The EHO algorithm demonstrated significant sustainability benefits per delivery cycle. Specifically, EHO achieved a 26.9% reduction in delivery distance (from ~5,200 km to ~3,800 km), a 26.9% reduction in fuel consumption (from ~520 liters to ~380 liters), and a 26.9% decrease in CO_2 emissions (from ~624 kg to ~456 kg). These improvements directly contribute to United Nations Sustainable Development Goals 11 and 13, promoting sustainable cities, communities, and climate action, thereby transforming logistics operations into a strategic tool for environmental stewardship.

From a computational perspective, EHO exhibits a time complexity of O(N × MaxIter × d), which is comparable to other swarm-based optimization algorithms. However, the empirical evaluations indicate that EHO converges approximately twice as fast as Particle Swarm Optimization (PSO), attributed to its phase-wise adaptive operators. Additionally, scalability tests reveal near-linear runtime growth for problems involving up to 100 cities, confirming EHO's efficiency for large-scale logistics optimization.

4.10 Limitations of the Proposed Framework

Despite its demonstrated performance, EHO has several practical limitations. First, the weighted-sum scalarization (Section III-A) requires objectives to be commensurable after normalization and while the sensitivity analysis in Section III-A indicates reasonable robustness, decision-makers with strongly asymmetric

priorities may prefer a full Pareto-front presentation (e.g., NSGA-II-style) rather than a single scalarized solution. Second, the emission model ($e_{ij} = 0.12 \cdot d_{ij}$) is a first-order approximation that does not yet account for vehicle load, congestion, or road gradient, which may affect emission estimates in dense urban corridors. Third, the current framework assumes a homogeneous vehicle fleet and a single depot; extending EHO to heterogeneous fleets and multi-depot configurations (identified as future work in Section V) would be required before industrial deployment at national scale. Finally, although the nineteen-city Egyptian network and the Solomon benchmark instances provide encouraging evidence of generalizability, further validation on larger-scale (100+ nodes) and internationally diverse networks is needed to confirm scalability claims beyond the near-linear trend observed up to a hundred cities.

5 Conclusion and Future Work

This research successfully developed, implemented, and validated the Enhanced Hippopotamus Optimization (EHO) algorithm for multi-objective physical distribution in smart supply chains. By mathematically modeling the social sophistication and survival behaviors of hippopotamuses—exploration, defensive coordination, and strategic retreat—EHO provides a powerful mechanism for balancing global exploration and local exploitation. Its integration with real-world geospatial data via the Google Maps API and stochastic demand modeling (Zipf distribution, $\alpha = 0.9$) ensures that solutions are both mathematically optimal and practically viable.

Extensive experimental results on a nineteen-city Egyptian network across twenty diverse scenarios demonstrated EHO's superiority over six state-of-the-art metaheuristics (PSO, GA, ACO, RUN, AO, FATA), achieving:

1. A26.9% reduction in distance, fuel consumption, and CO_2 emissions.
2. Fastest runtime (≈12.77 s) and lowest response time (≈120 ms).
3. High-quality Pareto-optimal solutions simultaneously minimizing distance, time, cost, and emissions.

These outcomes provide quantifiable evidence that EHO can meaningfully improve the economic efficiency and environmental sustainability of physical distribution, directly supporting UN SDGs 11 and 13. While these results are encouraging, they are based on a single national road network and a weighted-sum formulation, as discussed in Section IV-J; broader validation across heterogeneous fleets, multiple depots, and additional geographic contexts is needed before the framework can be considered industry-ready. The framework nonetheless represents a promising step toward green AI for logistics, offering an efficient and extensible foundation for future sustainable routing research.

Future work will focus on further enhancing EHO's applicability and scalability:

1. Dynamic Routing: Integrate real-time traffic and weather data to enable adaptive rerouting during delivery.
2. Fleet Heterogeneity: Extend the model to handle heterogeneous fleets with diverse capacities, fuel efficiencies, and emission profiles.
3. Multi-depot Systems: Optimize distribution from multiple depots simultaneously.
4. Hybridization: Combine EHO with exact methods (e.g., branch-and-bound) to guarantee optimality in large-scale problems.
5. Hardware Implementation: Develop dedicated hardware accelerators (e.g., FPGA) for real-time national-scale logistics optimization.

EHO thus represents a robust, efficient, and sustainable framework for intelligent logistics optimization, offering tangible benefits for businesses and policymakers seeking to enhance operational efficiency and achieve environmental sustainability.

Acknowledgements

The first author gratefully acknowledges the valuable contributions and support of the co-authors, Amal Elsayed Aboutabl, Naglaa Mohamed Diaa, and Riham Younis Haggag, throughout the development of this research. Their contributions to the research design, methodology, analysis, interpretation of results, and critical review of the manuscript are greatly appreciated and contributed significantly to the completion of this work.

References

[1] Amiri, M.H., Mehrabi Hashjin, N., Montazeri, M., Mirjalili, S. & Khodadadi, N., *Hippopotamus Optimization Algorithm: A Novel Nature-inspired Optimization Algorithm*, Sci. Rep., **14**(1), 5032, Dec. 2024. doi: 10.1038/s41598-024-5032-0.

[2] Chen, W., Men, Y., Fuster, N., Osorio, C. & Juan, A.A., *Artificial Intelligence in Logistics Optimization with Sustainable Criteria: A Review*, Sustainability, **16**(21), 9145, Oct. 2024. doi: 10.3390/su16219145.

[3] Shuaibu, A.S., Mahmoud, A.S. & Sheltami, T.R., *A Review of Last-mile Delivery Optimization: Strategies, Technologies, Drone Integration, and Future Trends*, Drones, **9**(3), 58, Feb. 2025. doi: 10.3390/drones9030158.

[4] Chau, M.L. & Gkiotsalitis, K., *A Systematic Literature Review on the Use of Metaheuristics for the Optimisation of Multimodal Transportation*, Evol. Intell., **18**(2), pp. 1–37, Jan. 2025. doi: 10.1007/s12065-024-01123-8.

[5] Kennedy, J. & Eberhart, R., *Particle Swarm Optimization*, in Proc. ICNN'95 - Int. Conf. Neural Netw., Perth, WA, Australia, **4**, pp. 1942–1948, Nov. 1995. doi: 10.1109/ICNN.1995.488968.

[6] Zhang, S., Lee, C.K.M., Chan, H.K., Choy, K.L. & Wu, Z., *Swarm Intelligence Applied in Green Logistics: A Literature Review*, Eng. Appl. Artif. Intell., **37**, pp. 154–169, Jan. 2015. doi: 10.1016/j.engappai.2014.09.014.

[7] Leng, J., Zhang, H., Yan, D., Liu, Q., Chen, X. & Zhang, D*., Digital Twin-Driven Manufacturing Cyber-physical System for Parallel Controlling of Smart Workshop*, J. Ambient Intell. Humaniz. Comput., **10**, pp. 1155–1166, Mar. 2019. doi: 10.1007/s12652-018-0854-1.

[8] Cancela, B., Morán-Fernández, L., Bolón-Canedo, V. & Alonso-Betanzos, A., *A Review of Green Artificial Intelligence: Towards a More Sustainable* Future, Neurocomputing, 128096, Mar. 2024. doi: 10.1016/j.neucom.2023.128096.

[9] Vijayakumar, S., *Optimization of Friction Stir Welding Parameters for Dissimilar Aluminium Alloys using RSM-GRA and RSM-TOPSIS: Towards Sustainable Manufacturing in Industry 4.0*, Results Eng., **27**, art. 107054, 2025. doi: 10.1016/j.rineng.2025.107054.

[10] Gugulothu, B., Bharadwaja, K., Vijayakumar, S., Rao, T.V.J., Sri, M.N.S., Anusha, P. & Agrawal, M.K., *Modeling and Parametric Optimization of Electrical Discharge Machining on Casted Composite using Central Composite Design*, Int. J. Interact. Des. Manuf., **18**(5), pp. 2793–2803, 2024. doi: 10.1007/s12008-023-01323-7.

[11] Karumuri, S., Haldar, B., Pradeep, A., Karanam, S.A.K., Sri, M.N.S., Anusha, P., Sateesh, N., Subbiah, R. & Vijayakumar, S., *Multi-objective Optimization using Taguchi based Grey Relational Analysis in Friction Stir Welding for Dissimilar Aluminium Alloy*, Int. J. Interact. Des. Manuf., **18**(3), pp. 1627–1644, 2024. doi: 10.1007/s12008-023-01529-9.

[12] Sivasundar, V., Kakkassery, J.J., Jaganathan, M., Satheesh Kumar, P.S., Vignesh, M. & Anbuchezhiyan, G., *ANN Modeling and Optimization of Friction Stir Welding Performance for AA6061 and AA5083 Alloy Joints*, Proc. Inst. Mech. Eng., Part L: J. Mater. Des. Appl., 2024. doi: 10.1177/09544089241283272.

[13] Sivasundar, V., Sri, M.N.S., Anusha, P., Gupta, D., Kumar, S., Kumar, N. & Ashok, N., *Predicting Wear Performance of Al6063 Hybrid Composites Reinforced with Multi-ceramic Particles using Experimental and ANFIS Approaches,* Eng. Rep., **7**(8), art. e70359, 2025. doi: 10.1002/eng2.70359.

[14] Sriram, D., Rao, V., Vijayakumar, S., Peyyala, A., Sri, M.N.S., Rao, N.S., Cheepurupalli, N. & Subbiah, R., *Microstructure, Mechanical Properties of Dissimilar Friction Stir Welded AA6063/AA5052 Alloys, and Optimization of Process Parameters using Box Behnken-TOPSIS*

Approach, Kovove Mater., **62**(6), pp. 363-375, 2024. doi: 10.31577/km.2024.6.363.

[15] Gugulothu, B., Anusha, P., Swapna Sri, M.N.S., Vijayakumar, S., Periyasamy, R. & Seetharaman, S., *Optimization of Stir-squeeze Casting Parameters to Analyze the Mechanical Properties of Al7475/B4C/Al2O3/TiB2 Hybrid Composites by the Taguchi Method*, Adv. Mater. Sci. Eng., 2022, art. 3180442, 2022. doi: 10.1155/2022/3180442.

[16] Anusha, P., Sri, M.N.S., Vijayakumar, S., Rao, T.V. Janardhana, Paramasivam, P., Jeyakrishnan, S. & Saxena, K.K., *Design and Optimization the Wear Characteristics for Al7178/TiO2/B4C/FA Central Hybrid Composite,* Int. J. Interact. Des. Manuf., **18**(8), pp. 5773-5781, 2024. doi: 10.1007/s12008-023-01341-5.

[17] Rajesh, M., Sri, M.N.S., Jeyakrishnan, S., Anusha, P., Manikanta, J.E., Sateesh, N., Nookaraju, B.C., Subbiah, R. & Vijayakumar, S., *Optimization Parameters for Electro Discharge Machining on Nimonic 80A Alloy using Grey Relational Analysis*, Int. J. Interact. Des. Manuf., 18(3), pp. 1429–1442, 2024. doi: 10.1007/s12008-023-01616-x.

[18] Dorigo, M. & Stützle, T., *Ant Colony Optimization*, MIT Press, Cambridge, MA, USA, 2004.

[19] Dadzie, E.B. & Richard, A., Evaluating the Role of Logistics in Supply Chain Management, Dama Acad. Scholarly J. Res., 10(1), pp. 112–133, Jan. 2025.

[20] Deb, K., Pratap, A., Agarwal, S. & Meyarivan, T., *A Fast and Elitist Multiobjective Genetic Algorithm: NSGA-II*, IEEE Trans. Evol. Comput., 6(2), pp. 182–197, Apr. 2002. doi: 10.1109/4235.996017.

[21] Abid, A., Yusuf, M. & Omar, L., *A Hybrid Green AI Model for CO2 Reduction in Last-mile Delivery*, Sustain. Cities Soc., 96, p. 104676, Sep. 2023. doi: 10.1016/j.scs.2023.104676.

[22] Ma, Z., Jen, C.-T., & Aazami, A., *Time-Dependent Vehicle Routing Optimization Incorporating Pollution Reduction Using Hybrid Gray Wolf Optimizer and Neural Networks*, Sustainability, **17**(11), 4829, 2025. https://doi.org/10.3390/su17114829.

[23] Sharma, B. & Natarajan, K., *Carbon-aware Adaptive Logistics Networks Using Green AI*, J. Clean. Prod., 409, p. 137259, Aug. 2024. doi: 10.1016/j.jclepro.2023.137259.

[24] Amini, M., Keshavarz, H. & Taheri, N., *Reinforcement Learning-based Sustainable Distribution Model with Dynamic Energy Pricing*, IEEE Access, 12, pp. 28445–28460, 2024. doi: 10.1109/ACCESS.2024.3321457.

[25] Rahman, S. & Al-Ghamdi, T., *Carbon-aware Path Planning Using Tabu-Enhanced GAI for Smart Cities*, Smart Transp. Infrastruct., 3(2), pp. 123–135, Jun. 2024. doi: 10.1016/j.sti.2024.04.002.

[26] Google Maps Platform, Directions API Documentation, Google, 2024. Available: https://developers.google.com/maps/documentation/directions, (8 October 2026).